288

.....contributing to man's
understanding of the environment world

SOURCE TIME FUNCTIONS AND SPECTRA FOR UNDERGROUND NUCLEAR EXPLOSIONS

D.H. VON SEGGERN
R.R. BLANDFORD
SEISMIC DATA LABORATORY

DECEMBER 17, 1971

Prepared for
AIR FORCE TECHNICAL APPLICATIONS CENTER
Washington, D.C.

Under
Project VELA UNIFORM

Sponsored by
ADVANCED RESEARCH PROJECTS AGENCY
Nuclear Monitoring Research Office
ARPA Order No. 1714

TELEDYNE GEOTECH
ALEXANDRIA LABORATORIES

APPROVED FOR PUBLIC RELEASE; DISTRIBUTION UNLIMITED.

DISCLAIMER NOTICE

THIS DOCUMENT IS THE BEST QUALITY AVAILABLE.

COPY FURNISHED CONTAINED A SIGNIFICANT NUMBER OF PAGES WHICH DO NOT REPRODUCE LEGIBLY.

Neither the Advanced Research Projects Agency nor the Air Force Technical Applications Center will be responsible for information contained herein which has been supplied by other organizations or contractors, and this document is subject to later revision as may be necessary. The views and conclusions presented are those of the authors and should not be interpreted as necessarily representing the official policies, either expressed or implied, of the Advanced Research Projects Agency, the Air Force Technical Applications Center, or the U S Government.

Unclassified
Security Classification

DOCUMENT CONTROL DATA - R&D
(Security classification of title, body of abstract and indexing annotation must be entered when the overall report is classified)

1. ORIGINATING ACTIVITY (Corporate author)
TELEDYNE GEOTECH
ALEXANDRIA, VIRGINIA

2a. REPORT SECURITY CLASSIFICATION
Unclassified

2b. GROUP

3. REPORT TITLE
SOURCE TIME FUNCTIONS AND SPECTRA FOR UNDERGROUND NUCLEAR EXPLOSIONS

4. DESCRIPTIVE NOTES (Type of report and inclusive dates)
Scientific

5. AUTHOR(S) (Last name, First name, Initial)
von Seggern, D.H.; Blandford, R.R.

6. REPORT DATE
17 December 1971

7a. TOTAL NO. OF PAGES
47

7b. NO. OF REFS
14

8a. CONTRACT OR GRANT NO.
F33657-72-C-0009

b. PROJECT NO.
VELA T/2706

c. ARPA Order No. 1714

d. ARPA Program Code No. 2E-10

9a. ORIGINATOR'S REPORT NUMBER(S)
288

9b. OTHER REPORT NO(S) (Any other numbers that may be assigned this report)

10. AVAILABILITY/LIMITATION NOTICES
Approved for public release; distribution unlimited.

11. SUPPLEMENTARY NOTES

12. SPONSORING MILITARY ACTIVITY
Advanced Research Projects Agency
Nuclear Monitoring Research Office
Washington, D.C.

13. ABSTRACT

The model of Haskell for explosion source time functions and spectra fails to satisfy data in the short-period band recorded teleseismically from the three Amchitka Island underground nuclear tests: LONG SHOT, MILROW and CANNIKAN. A more recent model due to Mueller and Murphy satisfies the data quite well. The difference in the two models is basically in the falloff at high frequencies. A simple revision of Haskell's model produces waveforms and spectra nearly identical to ones from Mueller and Murphy's model. This revision requires velocity waveforms to have a rise time of extremely short duration at the elastic boundary, a premise validated by actual near-field measurements.

Waveforms are derived from the revised Haskell model and the Mueller and Murphy model and illustrated for pressure at the elastic boundary, reduced displacement potential at the elastic boundary, and far-field displacement. Corresponding spectra are derived and illustrated.

14. KEY WORDS
Explosive Source Time Function
Explosive Source Spectra

Unclassified
Security Classification

SOURCE TIME FUNCTIONS AND SPECTRA FOR UNDERGROUND NUCLEAR EXPLOSIONS

SEISMIC DATA LABORATORY REPORT NO. 288

AFTAC Project No.:	VELA T/2706
Project Title:	Seismic Data Laboratory
ARPA Order No.:	1714
ARPA Program Code No.:	2F-10
Name of Contractor:	TELEDYNE GEOTECH
Contract No.:	F33657-72-C-0009
Date of Contract:	01 July 1971
Amount of Contract:	$ 1,314,000
Contract Expiration Date:	30 June 1972
Project Manager:	Royal A. Hartenberger (703) 836-7647

P. O. Box 334, Alexandria, Virginia

Approved for public release; distribution unlimited.

ABSTRACT

The model of Haskell for explosion source time functions and spectra fails to satisfy data in the short-period band recorded teleseismically from the three Amchitka Island underground nuclear tests: LONG SHOT, MILROW and CANNIKAN. A more recent model due to Mueller and Murphy satisfies the data quite well. The difference in the two models is basically in the falloff at high frequencies. A simple revision of Haskell's model produces waveforms and spectra nearly identical to ones from Mueller and Murphy's model. This revision requires velocity waveforms to have a rise time of extremely short duration at the elastic boundary, a premise validated by actual near-field measurements.

Waveforms are derived from the revised Haskell model and the Mueller and Murphy model and illustrated for pressure at the elastic boundary, reduced displacement potential at the elastic boundary, and far-field displacement. Corresponding spectra are derived and illustrated.

TABLE OF CONTENTS

LIST OF FIGURES

LIST OF FIGURES (Cont'd.)

LIST OF TABLES

SYNOPSIS OF PREVIOUS WORK ON SOURCE SPECTRA AND YIELD SCALING

The response of an infinite homogeneous elastic medium to a pressure function acting on the boundary of a spherical cavity has a well-known solution (e.g., Sharpe, 1942; Blake, 1952). The solution for simple time functions of pressure such as a step or a decaying pulse are straightforward. Recently attempts have been made to model the exact source time function for nuclear detonations with the aid of close-in empirical measurements. Among other reasons, we feel it is imperative to obtain a nearly exact model for the source function so that spectral ratios applied to the short-period band, from 0.2 to 5 cps, can be formed and analyzed in an intelligent manner for purposes of discrimination.

Haskell (1967) formulated the source spectrum of an explosion by fitting a parameterized function to actual displacement potential functions calculated from measurements just outside the elastic radius of underground nuclear explosions. The function used results in a far-field displacement spectrum which is asymptotic as the inverse of the fourth power of frequency (von Seggern and Lambert, 1970). This falloff entails a high-frequency scaling of displacement inversely proportional to the cube root of yield (i.e., large explosions emit less high frequency energy than small explosions) and a low-frequency scaling of displacement proportional to yield.

Mueller and Murphy (1971) have formulated a model based on theoretical considerations of the medium response to an explosive source near the surface. The theoretical underpinnings are basically those of Sharpe (1942) and Blake (1952). The far-field displacement spectrum from these models is asymptotic as the inverse of the square of frequency for high frequencies. This entails a high-frequency scaling of displacement directly proportional to the cube root of yield, in contrast to Haskell's model. The low-frequency scaling is the same as for Haskell's; that is, displacement is proportional to yield.

The purpose of this report is to compare the two models to data taken from teleseismic recordings of the three Amchitka Island underground tests. A full development of explosion functions will be made after reviewing the data; this will include representations for the pressure and displacement potential at the elastic radius of the explosion, the far-field displacement, and the spectrum of each of these functions. In this report we exclude the effects of the free surface on the theoretical source functions, and for comparison with theory we attempt to remove the free surface effects in the data.

BODY-WAVE SCALING FOR AMCHITKA ISLAND TESTS

Scaling of first motion amplitudes for LONG SHOT, MILROW, and CANNIKAN

We will compare the measured relative amplitudes of the P-wave for the three Amchitka Island tests with values calculated from the two theoretical scaling formulas under consideration. The reported yields of the three explosions are: LONG SHOT, 80 kt; MILROW, 1000 kt; CANNIKAN, 5000 kt. In order to avoid the effects of the reflection from the surface, which is delayed approximately a half second relative to the initial pulse for LONG SHOT (Cohen, 1969) and more for the other two shots, we must use the unbiased amplitudes of the initial upward ground motion at the receiver. By measuring this first quarter-cycle at several common stations, von Seggern and Lambert (1971) determined the ratio of MILROW to LONG SHOT amplitude to be 6.49. We have repeated the same procedure with CANNIKAN and MILROW at seven common stations for which data could be obtained at the Seismic Data Laboratory; the measurements are listed in Table I. The average ratio of CANNIKAN to MILROW amplitude is thus estimated to be 2.56.

From Haskell's scaling theory for granite, we can calculate using the displacement spectrum formula as given by von Seggern and Lambert (1970) the relative amplitudes at a frequency of one cps. From Haskell's work, one is not able to account for the effects of small changes in medium properties. The granite scaling

TABLE I

Station	Cannikan Milrow
LAO	2.59
KN	2.36
RK	2.63
CR	2.47
HN	2.01
BE	3.16
TFO	2.70
Average	2.56
Standard Deviation	.35

is used because the Amchitka tests apparently follow the "hard rock" magnitude-yield scaling at NTS (von Seggern and Lambert, 1971). The amplitude ratios are calculated at one cps because this agrees fairly well with the period of the first cycle of motion at all the stations for all three shots. There is a slight shift to lower frequencies for increasing yield though. The scaling ratio between two shots in granite at 1 cps is given by:

$$\frac{u_2}{u_1} = \frac{Y_2}{Y_1} \frac{[1 + 4\pi^2 G^2 Y_2^{2/3} A^2]^{1/2}}{[1 + 4\pi^2 G^2 Y_1^{2/3} A^2]^{1/2}} \frac{[1 + 4\pi^2 G^2 Y_1^{2/3}]^{5/2}}{[1 + 4\pi^2 G^2 Y_2^{2/3}]^{5/2}} \qquad (1)$$

where

u = vertical displacement in far field
Y = yield
G = .0185 - constant for granite
A = 1 + 24B
B = .24 - constant for granite.

Calculations using (1) give a ratio of MILROW to LONG SHOT amplitude of 6.58 and a ratio of CANNIKAN to MILROW amplitude of 1.51.

The scaling theory of Mueller and Murphy (1971) involves considerably more terms which must be estimated from available data. Their scaling relation between two shots in different media at different depths at 1 cps is given by:

$$\frac{u_2}{u_1} = \frac{r_{el_2}\, c_2 \mu_1}{r_{el_1}\, c_1 \mu_2} \cdot \left[\frac{\alpha_1^2 + 4\pi^2}{\alpha_2^2 + 4\pi^2}\right] \cdot \left[\frac{4\pi^2 p_{os_2}^2 + \alpha_2^2 p_{oc_2}^2}{4\pi^2 p_{os_1}^2 + \alpha_1^2 p_{oc_1}^2}\right]^{1/2}$$

$$\cdot \left[\frac{16\pi^4\beta_1^2 + (1-2\beta_1)4\pi^2\omega_{o_1}^2 + \omega_{o_1}^4}{16\pi^4\beta_2^2 + (1-2\beta_2)4\pi^2\omega_{o_2}^2 + \omega_{o_2}^4}\right]^{1/2} \qquad (2)$$

where

r_{el} = elastic radius
c = compressional-wave velocity
μ = rigidity modulus
ω_o = c/r_{el}
β = $(\lambda + 2\mu)/4\mu$ (λ is Lame's constant)
α = $k\omega_o$ (k being approximately 2 for granite)
p_{os} = 1.5 ρgh (ρ is density, g is gravitational acceleration, and h is depth)
p_{oc} = $(4\mu/3)(r_c/r_{el})^3$ (r_c is final cavity radius).

The value p_{os} is the initial pressure, and p_{oc} is the residual pressure at large t. Several assumptions must be made now. We first assume $\lambda = 2\mu$ thus making $\beta = 1$. This implies that Poisson's ratio is equal to .33, a value more suited to rocks at shallow depth than .25. We assume that r_{el} scales exactly as the cube root of yield, and that r_c/r_{el} equals 0.1. Both these assumptions are reasonable approximations (Mueller and Murphy, 1971). For the LONG SHOT site, we use c = 3.5 km/sec as indicated by the velocity log at the LONG SHOT site (Lambert et al., 1969). For the MILROW site, we use c = 4.0 km/sec as indicated by the velocity log prepared by Snyder (1969). We do not as yet know the

the velocity at the CANNIKAN site; but, using an accepted velocity-depth law of $v = v_0 + a(h-h_0)$ where v is the estimated velocity for the CANNIKAN test at 1.8 km depth, v_0 is the MILROW velocity at its 1.2 km depth, and $a = 1$ km/sec/km, we obtain a velocity of 4.6 km/sec for CANNIKAN. Using the relation $\lambda = 2\mu$, we can calculate the rigidity moduli for all three sites: LONG SHOT, 7.4; MILROW, 1.6; CANNIKAN, 12.7. To calculate the peak pressures, p_{os}, we use $\rho = 2.4$ gm/cc at all three sites as indicated by the fairly constant density-depth profile at the LONG SHOT site (Lambert et al., 1969). The remainder of the parameters in (2), α, ω_o, and p_{oc}, can now be calculated. Application of (2) then to the three tests results in predicted amplitude ratios of MILROW to LONG SHOT of 7.57 and of CANNIKAN to MILROW of 2.36.

Table II summarizes the observed and calculated amplitude ratios. Both the scaling relations of Haskell and Mueller and Murphy agree with the actual MILROW to LONG SHOT amplitudes quite well. For CANNIKAN to MILROW, however, Haskell's scaling is significantly in error while that of Mueller and Murphy agrees very well with the data. Together with the RK-ON spectral ratios for LONG SHOT/MILROW due to Sax (1972), it was in fact the failure of Haskell's scaling theory to correctly predict the CANNIKAN amplitude which initiated this study.

For three reasons the above comparisons cannot be entirely convincing in supporting Mueller and Murphy's scaling relation over Haskell's. Firstly, the change in the spectral shape with increasing yield in conjunction with the frequency response of the recording systems

TABLE II

	Milrow / Long Shot		Cannikan / Milrow	
	Ratio	Log (Ratio)	Ratio	Log (Ratio)
Measured Data	6.49	.81	2.56	.41
Haskell's Model	5.61	.75	1.28	.11
Mueller & Murphy's Model	7.57	.88	2.36	.37

may distort the measured relative amplitudes at 1 cps; however we have estimated that this effect cannot be more than 0.1 or 0.2 in the logarithm. Secondly, the number of assumptions and estimations required in applying Mueller and Murphy's scaling relation calls for considerable error limits on its results. Thirdly, Haskell's theory allows for no comparison between shots at different depths and in media other than the four which he examined and is therefore not a general scaling theory.

P-wave spectral ratios at RK-ON

To reinforce the results of the comparison using initial P-wave amplitude data, we will examine the entire short period band of the recorded P-waves from MILROW and LONG SHOT and compare this with spectral calculations from the two scaling relations.

Specifically, we examine the spectra of LONG SHOT and MILROW P waves at RK-ON as shown by von Seggern and Lambert (1971). These unsmoothed spectra are corrected for noise by subtracting out the spectrum of a noise sample just preceding the signals. RK-ON was chosen among the many stations in that report because the signal is above the noise out to 5 cps at least for LONG SHOT, and because the modulation of the spectra by the surface reflection is nearly ideally shown in both cases. We can remove the effect of the surface reflection when we merely smooth over these modulations by connecting adjacent spectral peaks with straight lines to get the spectra shown in Figure 1. From these smoothed spectra,

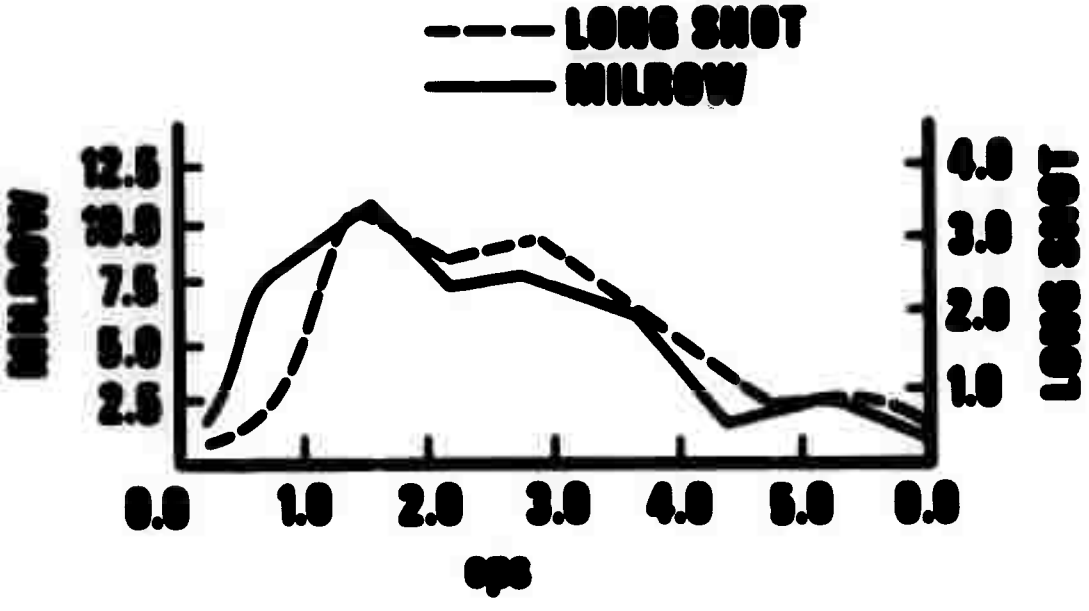

Figure 1. RK-0N smoothed acceleration spectra for MILROW and LONG SHOT.

we calculate amplitude ratios of MILROW to LONG SHOT at 0.5 cps intervals and plot them as in Figure 2. In addition, the amplitude ratio at long periods can be obtained from the match filter method for Rayleigh waves; von Seggern and Lambert report this to be 8.5 at [illegible], and we plot this at .05 cps in Figure 2. Using Haskell's scaling relation for 80 and 1000 kt shots in granite, we compute the spectral ratios shown in Figure 2. Using a revision of Haskell's model to give a falloff at high frequencies proportional to the inverse of frequency squared as in Mueller and Murphy's model, we calculate the ratios shown in Figure 2 which agree remarkably well with the actual data. (This revision will be discussed in the next section, but its form is nearly equivalent to Mueller and Murphy's, and a full extension of equation (2) across the band from 0.5 to 5 cps would produce a line nearly identical to the solid one shown in Figure 2.)

The results of comparing spectral ratios at one station and first motion amplitudes at several stations together affirm the validity of the model of Mueller and Murphy and cast doubt on the validity of Haskell's model. In the next section we will delineate the essential physical differences of the explosive source mechanism as inferred by the two models and develop general forms for representing the source time functions and spectra.

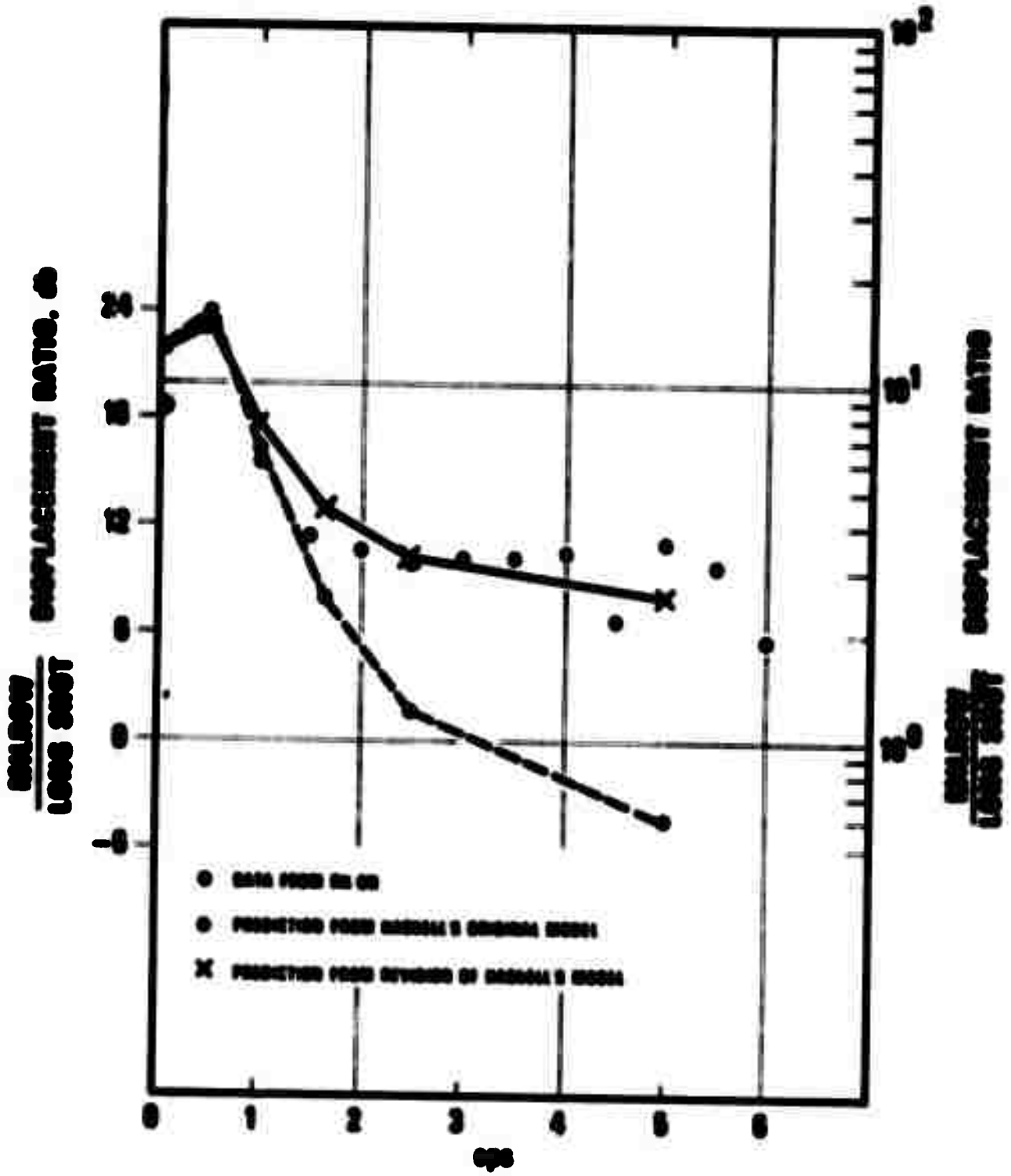

Figure 2. Theoretical and observed displacement ratios for Hilton and Long Shot.

GENERALIZED FORMS FOR EXPLOSIVE SOURCE TIME FUNCTIONS AND SPECTRA

Haskell's original formulation

Haskell (1967) formulated his model by fitting curves of the type

$$\frac{\psi(t)}{\psi(\infty)} = 1 - e^{-kt}\left[1 + kt + \frac{(kt)^2}{2} + \frac{(kt)^3}{6} - 8(kt)^4\right] \qquad (3)$$

where $\psi(\infty)$ is the asymptotic value for large t, to reduced displacement potentials calculated from data taken just outside the elastic radius of several underground nuclear detonations. As stated by him, the form of this function was chosen so as to make displacement, velocity, and acceleration functions continuous at t = 0 (t is the retarded time referred to the elastic boundary). This entails, as shown by von Seggern and Lambert (1970), the ω^{-4} dependence at high frequencies for the far-field displacement spectrum. Haskell's curves according to (3) are apparently excellent fits to the data he shows. We reproduce his example for a granite medium in Figure 3. However, note that at the beginning of the waveform, which is the critical area in relation to the falloff of the high-frequency portion of the spectrum, his analytic curve has a slope significantly less than the real slope. We feel that Haskell's requirement of continuous acceleration and velocity at the elastic radius is physically too strong, and therefore we can

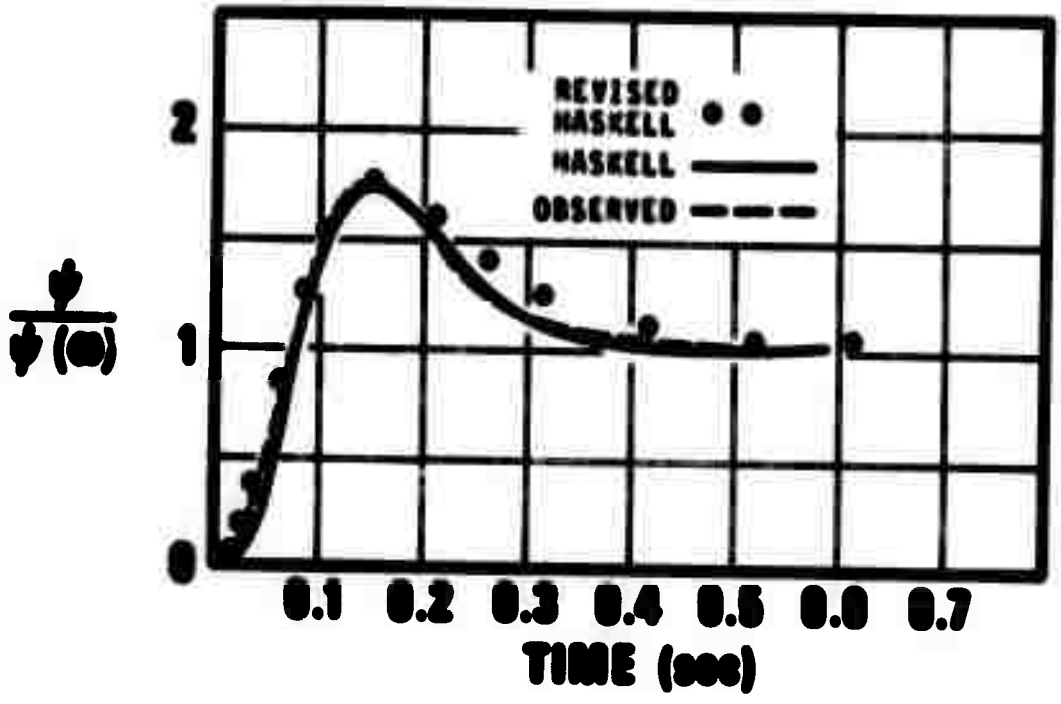

Figure 3. Observed and analytic displacement potentials for granite (from Haskell, 1967).

safely assume the more idealized case where acceleration and even velocity are discontinuous at the elastic boundary of the medium surrounding the explosion. These may not be the exact discontinuities, but the jump should occur in a time span which is nearly instantaneous relative to the frequency band under consideration. We show in Figure 4 a reproduction of a particle velocity measurement outside the elastic boundary of the GASBUGGY shot (Perret, 1960). The velocity takes a large initial jump in approximately .01 seconds; this implies that for frequencies less than approximately 100 cps, the spectrum is that of an impulse, i.e., flat. In contrast, Haskell would require particle velocity to be a ramp-like function which implies an ω^{-2} falloff for high frequencies in the spectrum.

Revision of Haskell's model

By removing the quartic and cubic terms from (3), we remove the constraints of continuous acceleration and velocity in the near field. Then we propose a source model by fitting the function

$$\frac{\dot{u}(t)}{\dot{u}(\infty)} = 1 - e^{-kt}[1 + kt - B(kt)^2] \qquad (4)$$

to the same data as used by Haskell. For the granite case in particular, we get values of $k = 16.8$ and $B = 2.04$ by requiring that (4) fit the peak of the

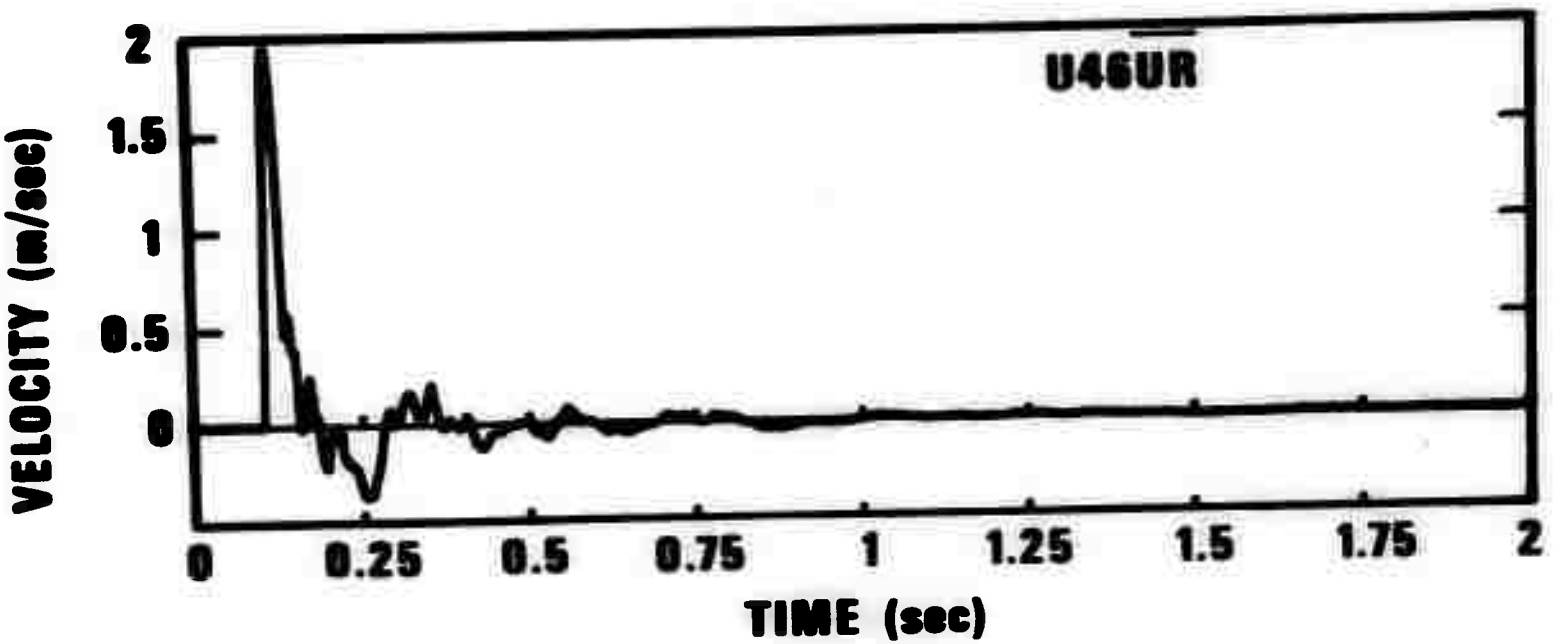

Figure 4. Particle velocity recording in near-field of GASBUGGY detonation (from Perret, 1969).

measured potential and the asymptotic long-term value $\psi(\infty)$. Several calculated points of this curve are shown in Figure 3.

The reduced displacement potential (4) and the pressure function on the elastic radius are related by (Rodean, equation 4.17):

$$\frac{r_{el}}{\rho\psi(\infty)}\,\sigma(t) = \frac{d^2\left[\frac{\psi(t)}{\psi(\infty)}\right]}{dt^2} + \frac{4b^2}{cr_{el}}\,\frac{d\left[\frac{\psi(t)}{\psi(\infty)}\right]}{dt} + \frac{4b^2}{r_{el}^2}\,\frac{\psi(t)}{\psi(\infty)} \quad . \tag{5}$$

Using (4) in (5), we obtain

$$\frac{r_{el}^3}{4\rho b^2\psi(\infty)}\,\sigma(t) = e^{-kt}[B(kt)^2 - Akt + 2B] + 1 \tag{6}$$

where $A = 2B + 1$, and we have assumed $k = c/r_{el}$ and, with $\lambda = 2\mu$, $k = 2b/r_{el}$. By equation 4.22 of Rodean (1971), we have for ω small in the frequency domain or t large in the time domain:

$$\psi(\infty) = \frac{r_{el}^3\, p_{oc}}{4\rho b^2} \tag{7}$$

Applying this relation to (6) results in:

$$\frac{1}{p_{oc}}\,\sigma(t) = e^{-kt}[B(kt)^2 - Akt + 2B] + 1 \tag{8}$$

if we continue the previous assumption of $\lambda = 2\mu$ and thus $c^2 = 4b^2$. We desire an expression for the far-field displacement also; this can be derived from the reduced displacement potential (4) if we employ this relation (Rodean, equation 4.16):

$$\frac{u(t)}{\psi(\infty)} = - \{\frac{1}{cr} \frac{d[\frac{\psi(t)}{\psi(\infty)}]}{dt} + \frac{1}{r^2} \frac{\psi(t)}{\psi(\infty)} \} \tag{9}$$

For the far-field displacement, we ignore the second term in (9) and thus have

$$\frac{cr}{\psi(\infty)} u(t) = - \frac{d[\frac{\psi(t)}{\psi(\infty)}]}{dt} \tag{10}$$

Substituting (4) in (10) then gives

$$\frac{rr_{el}}{\psi(\infty)} u(t) = kt\, e^{-kt}[A - Bkt] \tag{11}$$

where again $k = c/r_{el}$ is assumed.

Equations (8), (4), and (11) give the pressure, reduced displacement potential, and far-field displacement waveforms. The parameter k is medium dependent; and we assume as did Haskell, that it scales as the inverse cube root of the yield Y. B is a medium-dependent parameter

which defines the amount of overshoot in reduced displacement potential waveform. In Figure 5a, 5b, and 5c, we show (8), (4), and (11), respectively as a function of the dimensionless parameter kt for five values of B: 0, 1, 2, 3, and 4. The case B = 2 for the reduced potentials in Figure 5b closely corresponds with the fit of (4) to the granite data of Haskell in Figure 3 when B was calculated to be 2.04. It appears that equation (4) then can fit observed potentials as well as Haskell's original function, equation (3). Not only does the elimination of quartic and cubic terms from Haskell's function produce a more physically satisfying function as explained above, but it does so without suffering any loss of fitting capability.

Spectra of the above three functions for pressure at the elastic radius, reduced potential at this radius, and far-field displacement can be derived. We start with the reduced potential (4); the Fourier transform is straightforward, but tedious, and the final form only is given:

$$\frac{c}{r_{el}\psi(\infty)} |\psi(\omega)| = (\omega/k)^{-1} \frac{[A^2(\omega/k)^2 + 1]^{1/2}}{[(\omega/k)^2 + 1]^{3/2}} \qquad (12)$$

Rodean (equation 4.19) gives the relation between the pressure spectrum $\sigma(\omega)$ and $\psi(\omega)$ as

$$\sigma(\omega) = \frac{\rho}{r_{el}} [k^2 - \omega^2 + i\omega k] \psi(\omega) \qquad (13)$$

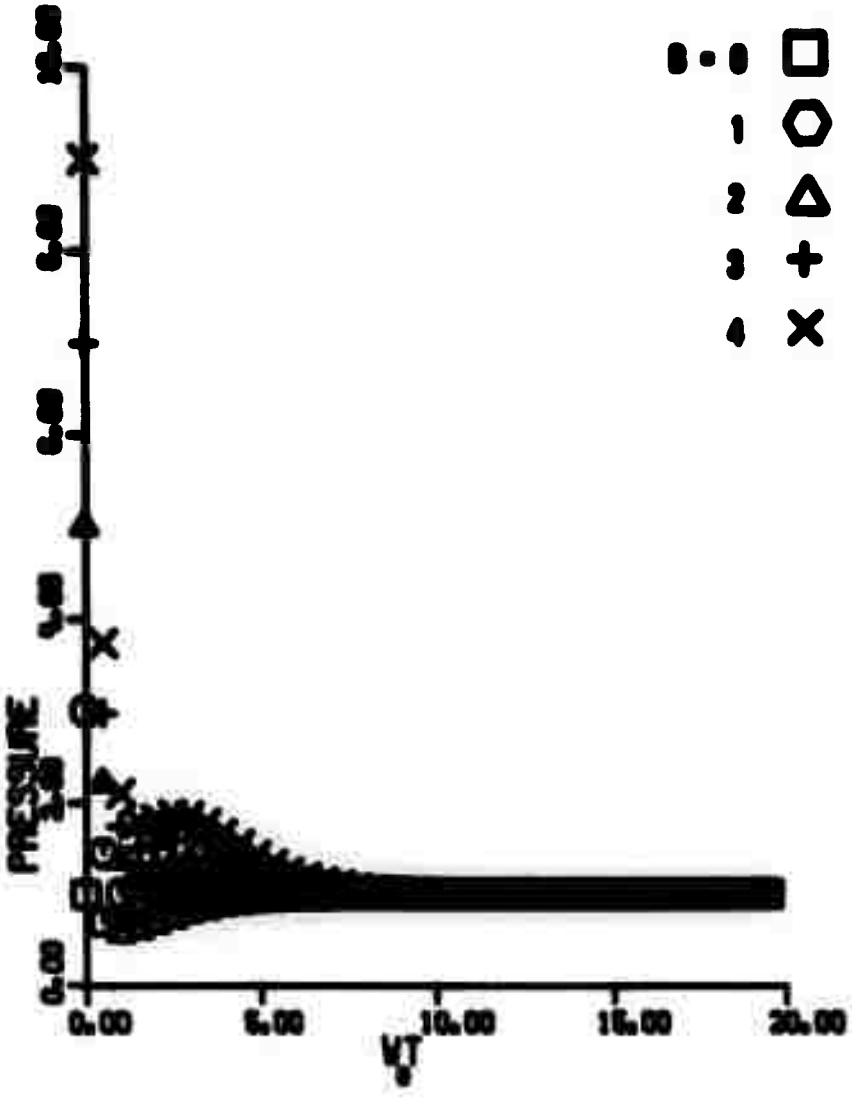

Figure 5a. Pressure waveforms at the elastic boundary calculated from revised Haskell's model.

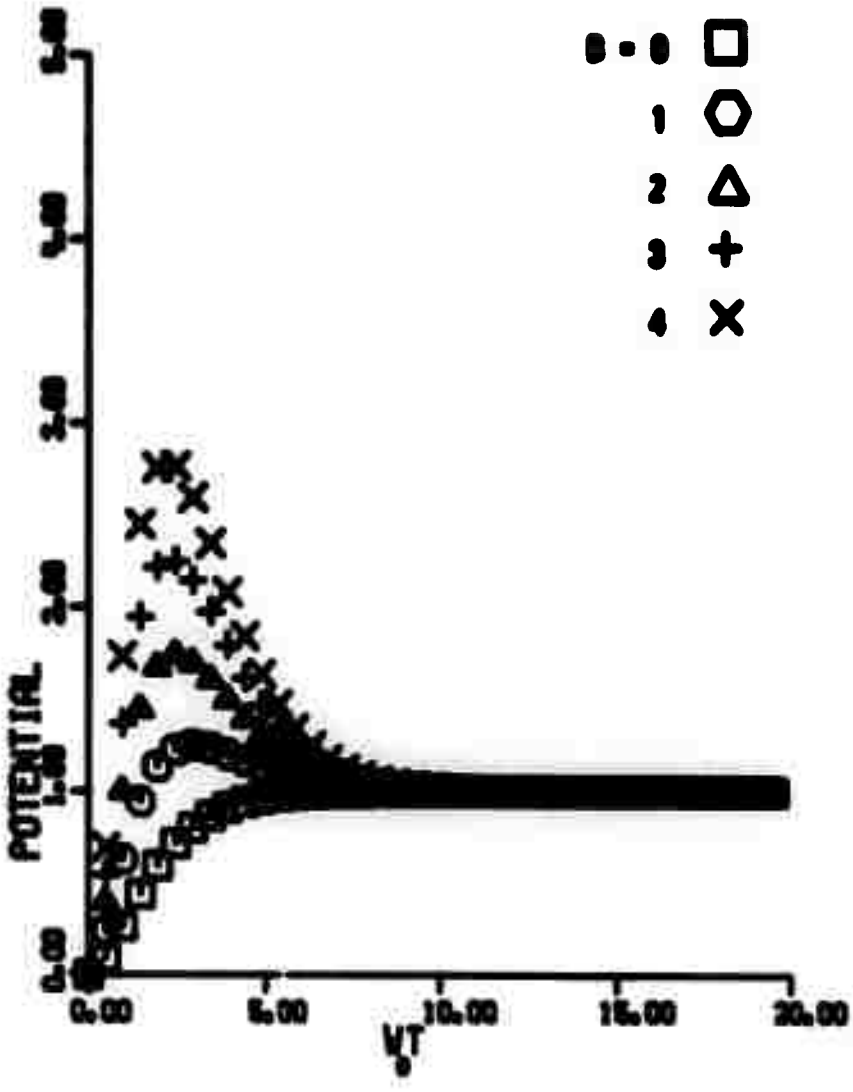

Figure 5b. Reduced displacement potential waveforms at the elastic boundary calculated from revised Haskell's model.

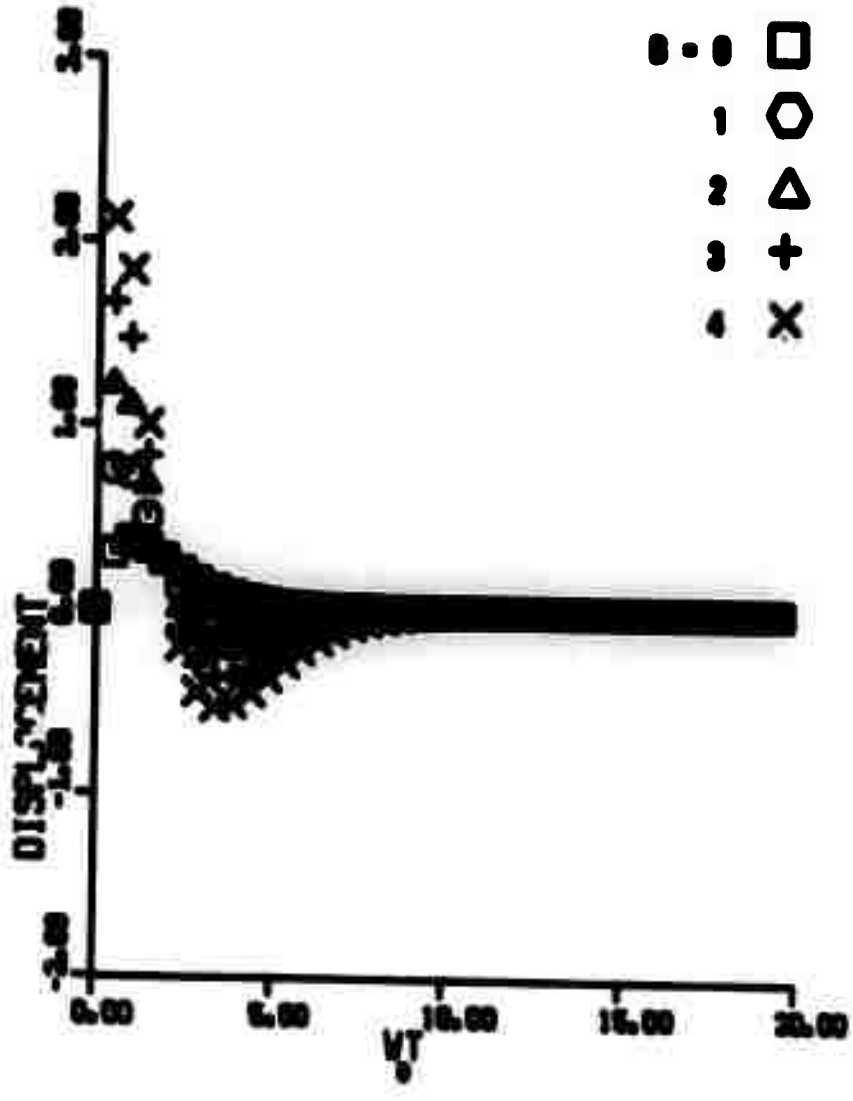

Figure 5c. Far-field displacement waveforms calculated from revised Haskell's model.

The modulus of this expression is

$$|\sigma(\omega)| = \frac{\rho}{r_{el}} \left[(k^2 - \omega^2)^2 + (\omega k)^2\right]^{1/2} |\psi(\omega)| \tag{14}$$

Substituting (12) in (14) and again using $k = c/r_{el}$ and the relation (7), we have

$$\frac{c}{\beta_{oc} r_{el}} |\sigma(\omega)| = (\omega/k)^{-1} \frac{\left[A^2(\omega/k)^2 + 1\right]^{1/2}}{\left[(\omega/k)^2 + 1\right]^{3/2}} \left\{\left[1 - \left(\frac{\omega}{k}\right)^2\right]^2 + \left(\frac{\omega}{k}\right)^2\right\}^{1/2} \tag{15}$$

The far-field displacement spectra can be derived with the aid of

$$\frac{|u(\omega)|}{\psi(\omega)} = -\frac{\omega}{cr} \frac{|\psi(\omega)|}{\psi(\omega)} \tag{16}$$

which is the modulus of the Fourier transform of (10). Using (16) in (12), we obtain

$$\frac{cr}{\psi(\omega)} |u(\omega)| = \frac{\left[A^2(\omega/k)^2 + 1\right]^{1/2}}{\left[(\omega/k)^2 + 1\right]^{3/2}} \tag{17}$$

if we again use $k = c/r_{el}$. Plots of (12), (15), and (17) are given in Figures 6a, 6b and 6c, respectively, as

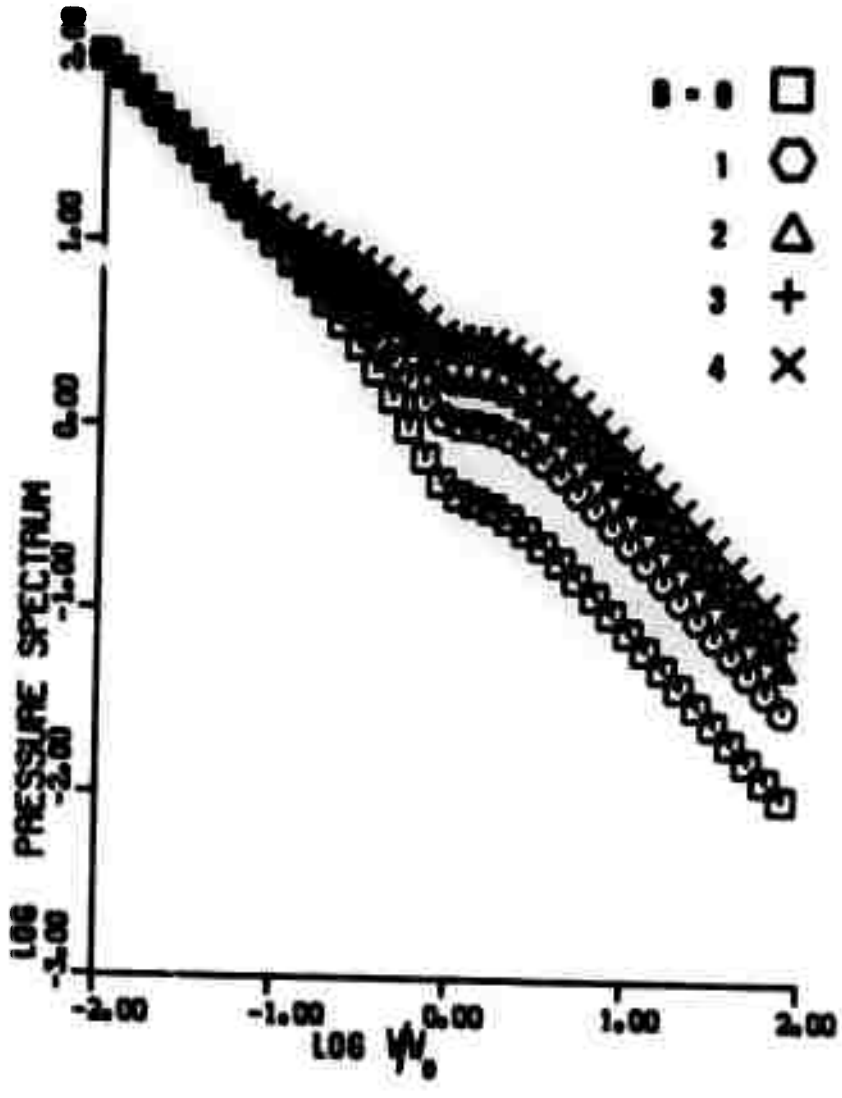

Figure 6a. Pressure spectra at the elastic boundary calculated from revised Haskell's model.

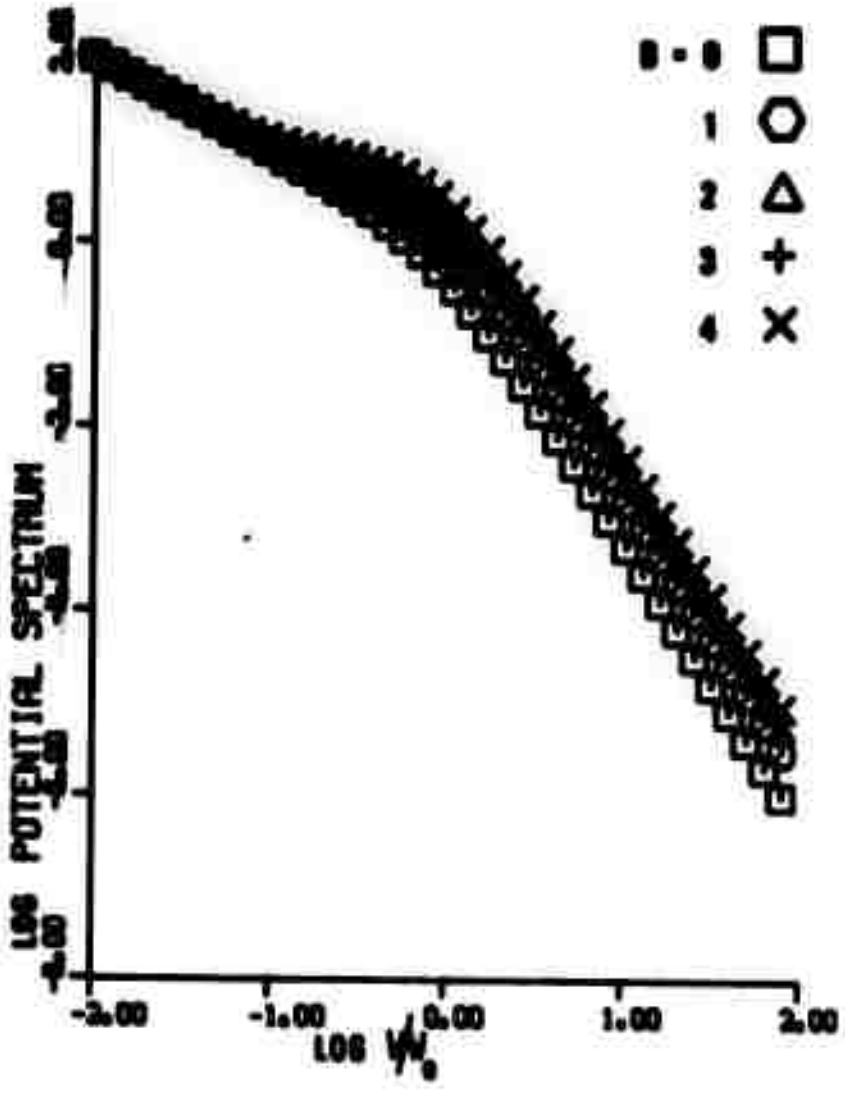

Figure 6b. Reduced displacement potential spectra at the elastic boundary calculated from revised Haskell's model.

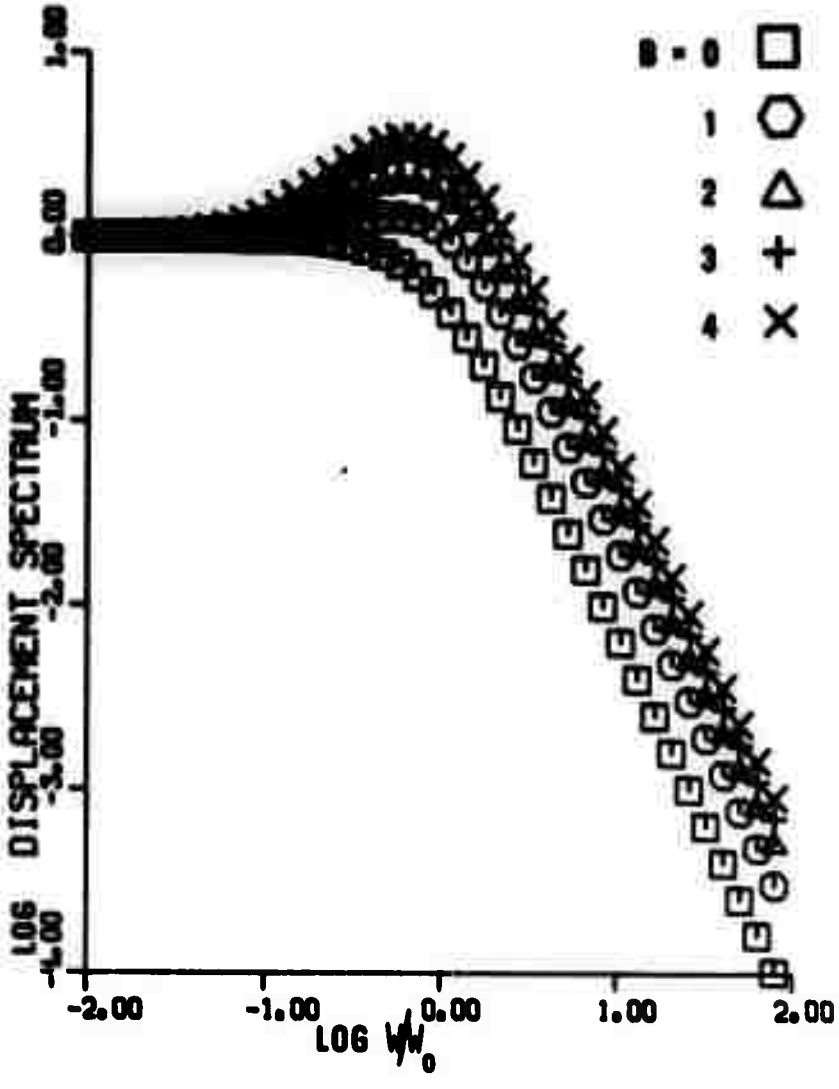

Figure 6c. Far-field displacement spectra calculated from revised Haskell's model.

functions of the dimensionless parameter ω/k for B values of 0, 1, 2, 3, and 4. Note that the required ω^{-2} falloff of the displacement spectra at high frequencies is present and that the overshoot in the displacement spectra is proportional to B.

Mueller and Murphy's formulation

Mueller and Murphy (1971) take a slightly different approach in deriving scaling relations. They assume the arbitrary form

$$\frac{1}{p_{oc}}\sigma(t) = p\, e^{-\alpha\omega_o t} + 1 \tag{18}$$

for the pressure at the elastic radius where $p = p_o/p_{oc}$ and $p_o = p_{os} - p_{oc}$ (p_{os} and p_{oc} are defined as for equation (2)) whereas Haskell began with an arbitrary form for reduced displacement potential. To derive the reduced displacement potential from the pressure function, we transform (18) into the frequency domain, apply equation (13), and inverse transform back to the time domain to get the reduced potential function. Inverse transforms #.011 and #.101 in Nixon (1960) are employed with the damping coefficient set to one-half. The reduction is straightforward, but again tedious, and we give only the final result:

$$\begin{aligned}\frac{1}{\psi(\infty)}\psi(t) = e^{-\omega_o t/2}\{.577[\frac{p(2\alpha-1)}{1-\alpha+\alpha^2} - 1]\sin(.866\omega_o t) \\ - [\frac{p}{1-\alpha+\alpha^2} + 1]\cos(.866\omega_o t)\} \\ + \frac{p}{1-\alpha+\alpha^2}e^{-\alpha\omega_o t} + 1\end{aligned} \tag{19}$$

The far-field displacement is obtained by use of (10) as before:

$$\frac{rr_{01}}{\psi(\infty)}\,u(t) = e^{-\omega_0 t/2}\left\{\frac{p\alpha}{1-\alpha+\alpha^2}\cos(.866\omega_0 t) - 1.154\left[\frac{p(\alpha/2-1)}{1-\alpha+\alpha^2} - 1\right]\sin(.866\omega_0 t)\right\} - \frac{p\alpha}{1-\alpha+\alpha^2}\,e^{-\alpha\omega_0 t} \qquad (20)$$

The pressure (18) could be plotted as a function of the dimensionless parameter $\alpha\omega_0 t$, but the reduced displacement potential (19) and the far-field displacement (20) cannot. Thus in fitting observed reduced potentials, Mueller and Murphy's formulation requires the additional parameter α to be estimated. The parameter $\alpha\omega_0$ corresponds to k in Haskell's formulation, and the parameter p here corresponds to his 2B. In Figures 7a, 7b and 7c, we show the plots of (18), (19), and (20), respectively, as a function of $\omega_0 t$ for $\alpha = 2$ when p is assigned values of 0, 1, 2, 3, and 4. Several other values of α were used, but $\alpha = 2$ is the value Mueller and Murphy suggest for rhyolite, which is compositionally close to granite. For $\alpha = 2$ and $p = 4$ in the reduced potentials of Figure 7b, the curve closely corresponds to the revised Haskell potential in Figure 5b when B is taken to be 2, approximately the value we obtained when fitting (4) to the granite data shown in Figure 3. This shows the analogy of p to 2B.

Spectra of the above functions for Mueller and Murphy's model can be obtained by starting with the easily transformable pressure function (18). The resulting pressure spectrum is:

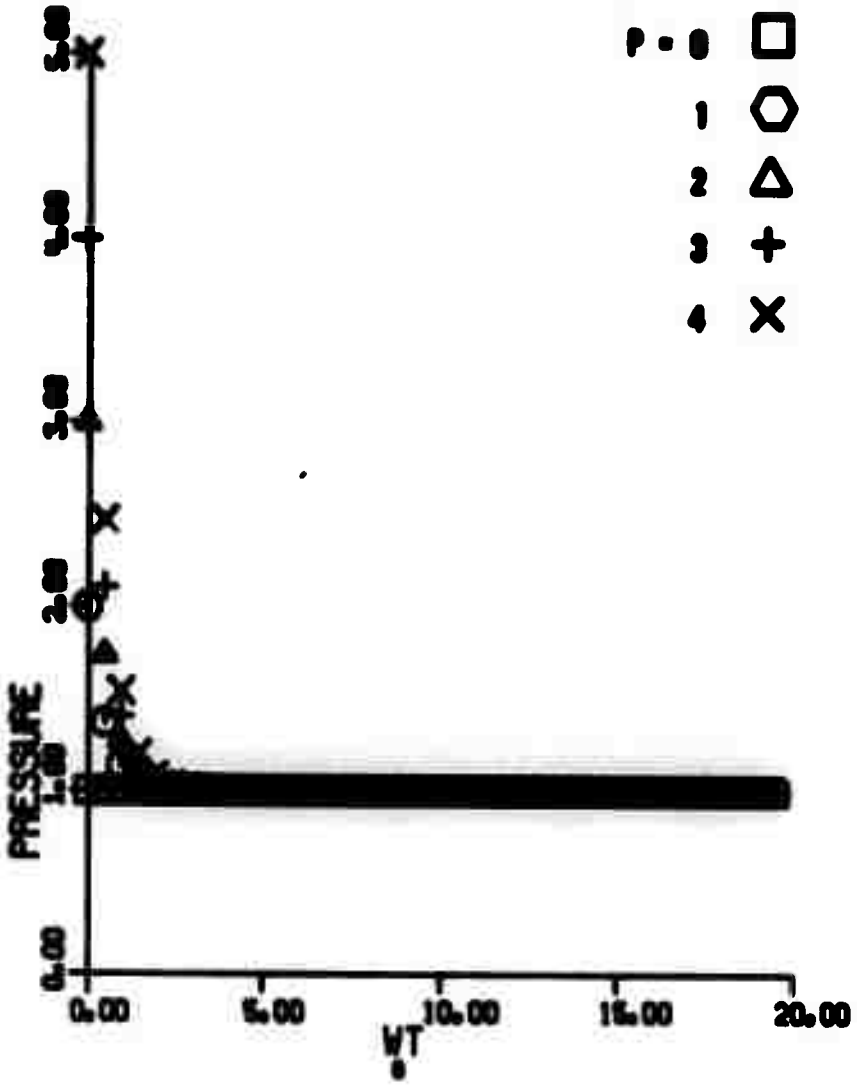

Figure 7a. Pressure waveforms at the elastic boundary calculated from Mueller and Murphy's model.

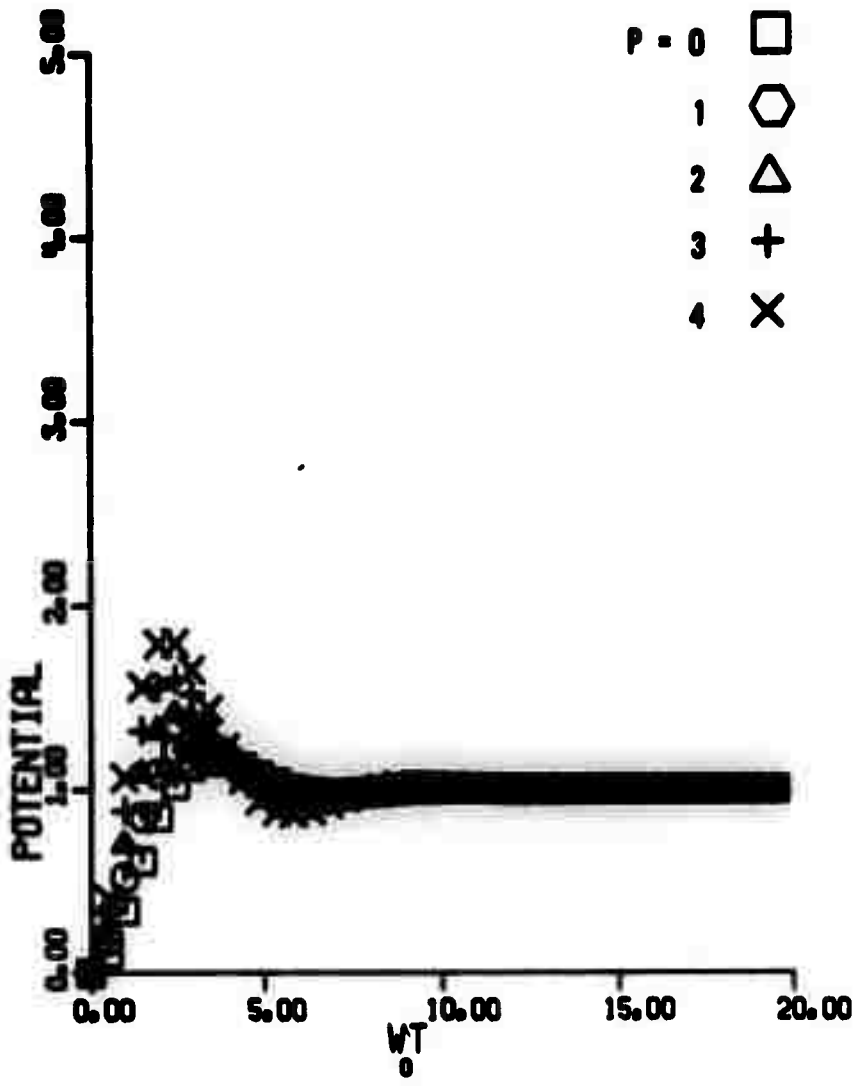

Figure 7b. Reduced displacement potential waveforms at the elastic boundary calculated from Mueller and Murphy's model.

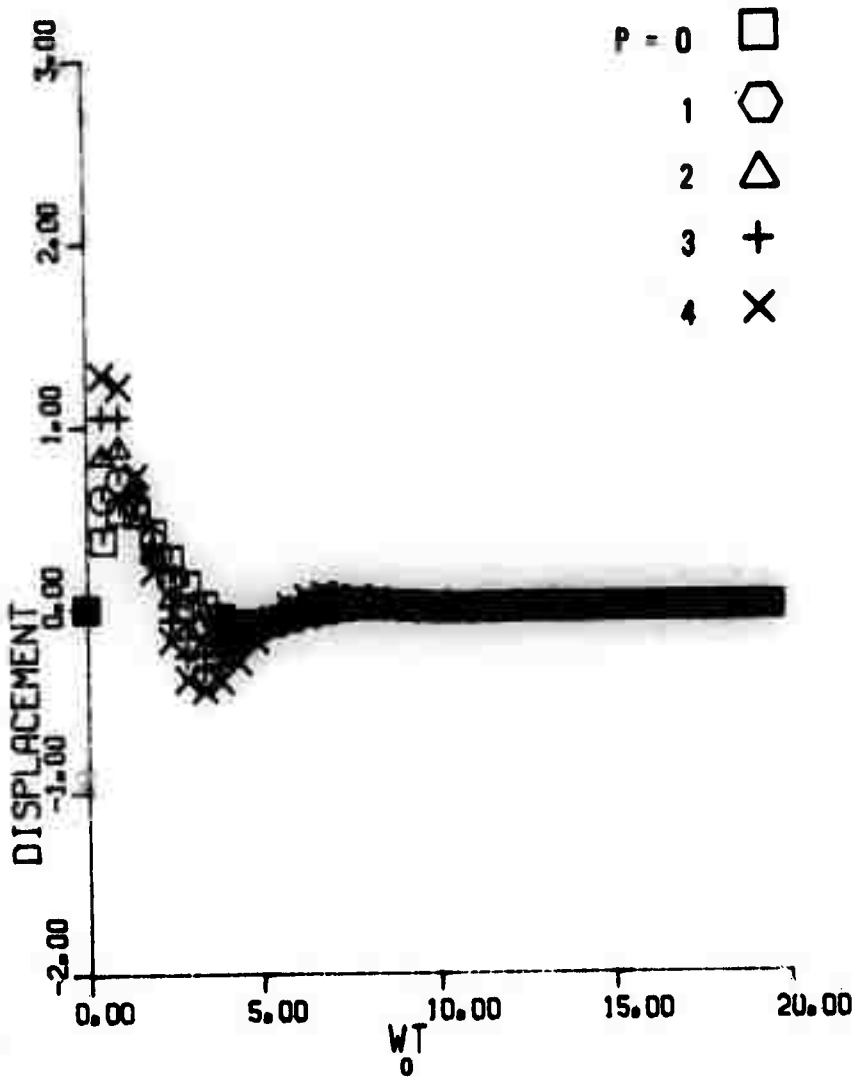

Figure 7c. Far-field displacement waveforms at the elastic boundary calculated from Mueller and Murphy's model.

$$\frac{c}{p_{oc}\, r_{el}} \left|\sigma(\omega)\right| = (\omega/\omega_o)^{-1} \left[\frac{(p+1)^2(\omega/\omega_o)^2 + \alpha^2}{(\omega/\omega_o)^2 + \alpha^2}\right]^{1/2} \tag{21}$$

The reduced potential spectrum follows by application of (14):

$$\frac{c}{r_{el}\psi(\infty)} \left|\psi(\omega)\right| = (\omega/\omega_o)^{-1} \left[\frac{(p+1)^2(\omega/\omega_o)^2 + \alpha^2}{(\omega/\omega_o)^2 + \alpha^2}\right]^{1/2} \cdot \left\{\left[1 - \left(\frac{\omega}{\omega_o}\right)^2\right]^2 + \left(\frac{\omega}{\omega_o}\right)^2\right\}^{-1/2} \tag{22}$$

The far-field displacement spectrum follows from (22) by application of (16):

$$\frac{cr}{\psi(\infty)} \left|u(\omega)\right| = \left[\frac{(p+1)^2(\omega/\omega_o)^2 + \alpha^2}{(\omega/\omega_o)^2 + \alpha^2}\right]^{1/2} \cdot \left\{\left[1 - \left(\frac{\omega}{\omega_o}\right)^2\right]^2 + \left(\frac{\omega}{\omega_o}\right)^2\right\}^{-1/2} \tag{23}$$

Note that, as for the corresponding time functions, the pressure spectrum (21) could be manipulated to be a function of the variable $\alpha\omega/\omega_o$ whereas the reduced potential spectrum (22) and displacement spectrum (23) cannot. In Figures 8a, 8b, and 8c we plot (21), (22), and (23), respectively, for $\alpha = 2$ with p set from 0 to 4 again. Comparison of Figure 8c with $p = 4$ to Figure 6c with $B = 2$ shows the similarity of the revised Haskell model and the Mueller and Murphy model for a granite-rhyolite medium.

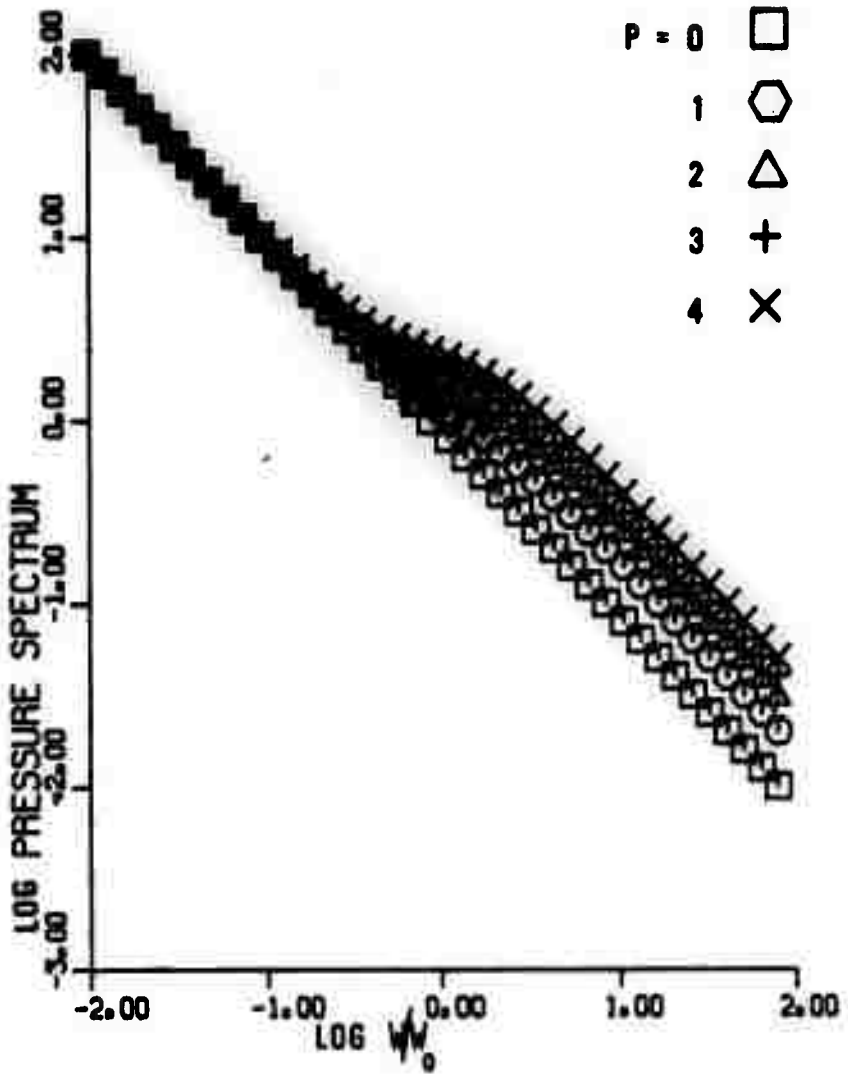

Figure 8a. Pressure spectra at the elastic boundary calculated from Mueller and Murphy's model.

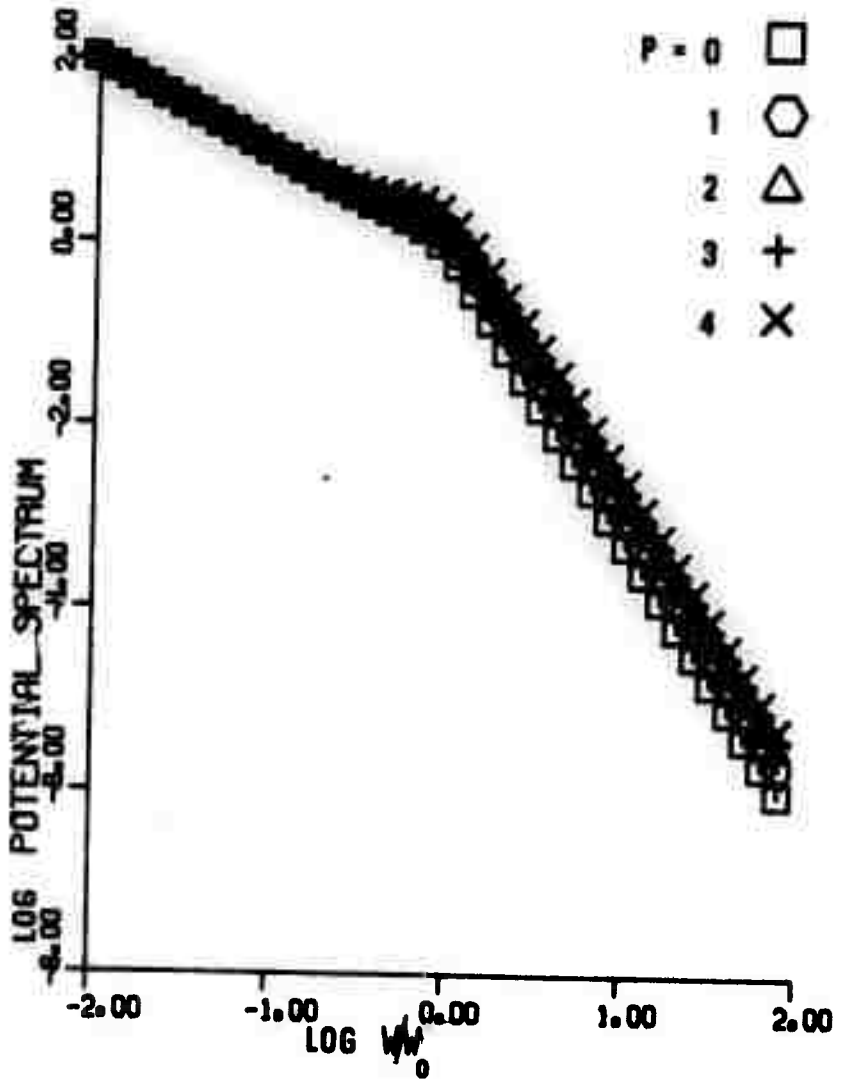

Figure 8b. Reduced displacement potential spectra at the elastic boundary calculated from Mueller and Murphy's model.

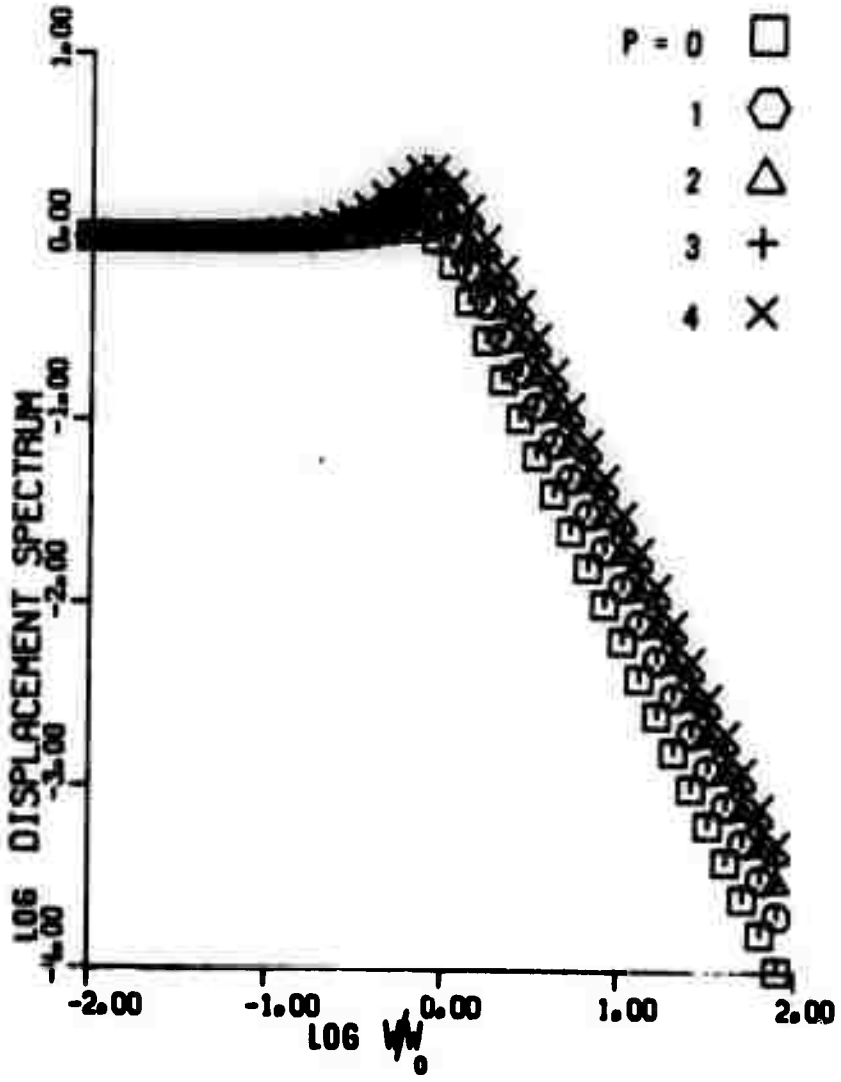

Figure 8c. Far-field displacement spectra calculated from Mueller and Murphy's model.

DISCUSSION

Using teleseismic data, we have shown that a model for the explosion source function which entails a far-field displacement spectrum that is inversely proportional to ω^2 at high frequencies is the proper choice. Mueller and Murphy (1971) have already verified this model using near-field data. Haskell's requirement that acceleration and velocity to be continuous at the elastic boundary around the explosion is unnecessary; they certainly can be considered as discontinuous for any part of the spectrum capable of being measured teleseismically. We mention that the ω^{-2} dependence at high frequencies is characteristic of earthquake models also (Aki, 1967; Brune, 1970).

We have revised Haskell's formulation to obtain an ω^{-2} model and found that the fit to observed potentials is apparently as good as with his original ω^{-4} model. We have used Mueller and Murphy's formulation for the pressure function at the elastic radius to derive reduced potential and far-field displacement waveforms. Waveforms and spectra for the two ω^{-2} models are similar. Observed waveforms can be fit by adjusting the parameters in either model, and this will be the subject of a future report. Especially important is estimation of the parameter p (or B) which is the ratio of the overshoot pressure p_o to the residual pressure p_{oc} at the elastic boundary. This value controls the peak in the far-field spectra and affects spectral ratios in the band around 1 cps. These pressures can be estimated

using the relations in equation (2) as taken from Mueller and Murphy. The parameter ω_o also controls the spectral shape near 1 cps, but its affect is predictable since $\omega_o = c/r_{el}$ and r_{el} scales as the cube root of yield when detonation depths are equal (Mueller and Murphy, 1971).

REFERENCES

Aki, Keiiti, 1967, Scaling law of seismic spectrum, J. Geophys. Res., v. 72, p. 1217-1232.

Blake, F.G., J4., 1952, Spherical wave propagation in solid media, J. Acoust. Soc. Amer., v. 24, p. 211-215.

Brune, James N., 1970, Tectonic stress and the spectra of seismic shear waves from earthquakes, J. Geophys. Res., v. 75, p. 4997-5009.

Cohen, T.J., 1970, Source-depth determinations using spectral, pseudo-autocorrelation, and cepstral analysis, Geophys. J.R. Astr. Soc., v. 20, p. 223-231.

Haskell, N.A., 1967, Analytic approximation for the elastic radiation from a contained underground explosion, J. Geophys. Res., v. 72, p. 2583-2587.

Lambert, D.G., von Seggern, D.H., Alexander, S.S. and Galat, G.A., 1969, The LONG SHOT experiment, Volume II: Comprehensive analysis, Seismic Data Laboratory Report No. 234, Teledyne Geotech, Alexandria, Virginia.

Mueller, Richard A. and Murphy, John R., 1971, Seismic characteristics of underground nuclear detonations: Part I, Seismic scaling law of underground detonations, Bull. Seismol. Soc. Amer., v. 61, p. 1675-1692.

Perret, William R., 19.., Project GASBUGGY: GASBUGGY seismic source and surface motion, Sandia Laboratories.

Rodean, Howard C., 1971, Nuclear-Explosion Seismology, U.S. Atomic Energy Commission, Division of Technical Information.

Sax, R.L. and Nelson, D.D., 1972, Application of source theory to Aleutian earthquake and explosion, Seismic Data Laboratory Report No. 289, Teledyne Geotech, Alexandria, Virginia.

Sharpe, J.A., 1942, The production of elastic waves by explosion pressures, I. Theory and empirical field observations, Geophysics, v. 7, p. 144-154.

Snyder, Richard P., 1969, Preliminary lithologic log of drill hole UAc-2 from 0 to 3,580 feet, Amchitka Island, Alaska, United States Geological Survey Report No. 474-52 (Amchitka-10).

von Seggern, David and Lambert, D.G., 1970, Theoretical and observed Rayleigh-wave spectra for explosions and earthquakes, J. Geophys. Res., v. 75, p. 7382-7402.

von Seggern, D.H. and Lambert, D.G., 1971, Analysis of teleseismic data for the nuclear explosion MILROW, Seismic Data Laboratory Report No. 258, Teledyne Geotech, Alexandria, Virginia.